JOURNAL OF PROPULSION AND POWER
Vol. 17, No. 3, May–June 2001

Thermal Choking Analyses in a Supersonic Combustor

M. G. Owens,* S. Mullagiri,* and C. Segal†
University of Florida, Gainesville, Florida 32611-6250
and
P. J. Ortwerth‡ and A. B. Mathur§
Boeing Defense and Space Group, Canoga Park, CA 91309-7922

The heat-release efficiency and the dynamics of thermal choking of a hydrogen-fueled supersonic combustor model have been evaluated in the low-speed flight regime characterized by Mach 3.75 flight enthalpy. The combustion chamber entrance Mach number, stagnation temperature, and combustor entrance Reynolds number were 1.56, 850 K and 1.2 million, respectively. The total equivalence ratio ranged to $\phi = 0.7$. A step-flameholding geometry was chosen to explore the effects of supersonic flow and high Reynolds number on normal bluff-body flame propagation and combustion efficiency using direct fuel injection from the base. The combustor was divided into two zones: a constant-area duct and an expanding section. The fuel was distributed in 1) the subsonic region formed in the base of the flameholder and 2) parallel to the main airflow in the core of streamwise vortices formed by the presence of ramps. In terms of fuel distribution, the split between the base and the ramp injectors over a range of total equivalence ratios indicated preference for the base injection at high total equivalence ratios. At modest total equivalence ratios no preferential fuel distribution among the injectors was found. Significant effects of compressibility and Reynolds number were found when compared to a reference experiment at low speed and low Reynolds number with the same step area ratio.

Nomenclature

A	=	area, mm^2
F_c	=	nozzle stream thrust, N
H	=	step height, mm
M	=	Mach number
$\dot{m}$	=	mass-flow rate, kg/s
P	=	static pressure, Pa
P_r	=	pressure ratio
P_s	=	wall pressure at $X/H = -12.92$, used for normalization, Pa
P^*	=	theoretical choking pressure, Pa
Re	=	Reynolds number
V	=	velocity, m/s
X	=	streamwise location, mm
η	=	combustion efficiency

Subscripts

b	=	base
c	=	combustor
i	=	nr. of injection ports
n	=	normal
r	=	ramp

Introduction

EFFICIENT heat release in supersonic combustion chambers requires fuel-injection schemes that offer rapid mixing with minimal pressure losses. The problem of achieving a high degree of fuel-air mixing in supersonic flows and the required length of mixing has received considerable attention with several mixing enhancing mechanisms studied to date. These include various injection configurations and generation of fluid mechanics interactions that enhance mixing, e.g., shocks,[1] vorticity,[2] and swirl motion.[3]

For high-speed applications parallel injection is preferred over transverse injection because of reduced pressure losses and thrust. Inflow-placed struts[4,5] provide a good fuel distribution along the entire airflow cross section, but are intrusive, thus inducing pressure losses[6] and raising cooling problems at high-speed flight conditions. Among proposed mixing configurations straight or swept ramps have shown good far-field mixing[7–10] despite reduced near-field mixing when compared with transverse injection. The ramp axial vortex shedding provides a mechanism that lifts the fuel from a low-injection angle and promotes fuel penetration into the core airstream thus enhancing mixing.

Often the suggested configurations feature a sudden expansion to separate the upstream flow from the pressure raise in the combustion chamber. In these cases it has been shown that mixing is largely dependent on the development and propagation of large-scale structures and the convection of flames initiated in the shear layers. In this regard previous works reporting experimental studies[11,12] of premixed two-dimensional flames formed the basis of the current approach. References 11 and 12 used burners with sudden expansions forming a rearward-facing step with an area ratio of 2 to 1 and an axial length of eight step heights, $8H$. These experiments used premixed gases with equivalence ratio $\phi = 0.57$, subsonic entrance velocity, and Reynolds number based on step height ranging between 2.2×10^4–3.7×10^4. The main emphasis was on analyses of kinematic data and the development of large-scale structures.

The differences in initial conditions between the current study and the experiments in Ref. 12 are significant. In particular, the Mach number in the present work is 1.56 compared to 0.07 in Ref. 12 and the Reynolds number $Re = 1.2 \times 10^6$ compared to 1.5×10^4. The equivalence ratio range in the current work overlaps the values used in Ref. 12, but the current study involves nonpremixed systems in contrast to the premixed flow in Ref. 12. The high-speed experiments presented herein have been designed to complement this low-speed database at similar overall equivalence ratio. A large favorable pressure gradient, expected in the current high-speed case near thermal choking condition, adds another significant difference. The acceleration caused by this pressure gradient is responsible for the propagation of the shear layer flame downstream of the reattachment. The velocity data in Ref. 12 indicated no acceleration of the cold

Received 1 January 2000; revision received 1 October 2000; accepted for publication 18 December 2000.

*Graduate Research Assistant, Department of Aerospace Engineering, Mechanics, and Engineering Science.
†Associate Professor, Department of Aerospace Engineering, Mechanics, and Engineering Science. Member AIAA.
‡Project Manager. Member AIAA.
§Process Leader. Member AIAA.

gas and only a moderate increase of gases flame velocity with no high-speed layer formation on the burned gas side. A discussion of previous work and the contribution of the shear layers to the development of the flow structures in reacting flows follows.

The main objective of the current study was to map the performance of the combined injection scheme on the fuel modulation between the two injection zones and overall fuel-air ratio with, 1) direct injection in the subsonic recirculation region to take advantage of the local low flow speed to improve the uniformity of the mixture in the flame propagating from the step and to achieve fast heat release at low flight enthalpy and 2) from supersonic injectors in the ramps that would benefit from improved mixing via axial vorticity from the supersonic side. Thus synergistic effects exist when both injection zones are used simultaneously. Hydrogen has been used as fuel with total equivalence rations to $\phi = 0.7$. The experimental conditions were fixed to correspond to flight enthalpies of Mach 3.5 at stagnation temperature of 850 K. The isolator entrance Mach number was fixed at 1.56.

Background

References 11 and 12 used flow visualization and laser Doppler velocimetry in nonreacting and chemically reacting flows to identify the effects of heat release on the velocity fields, reattachment length, and the flame propagation rate. In these studies[11,12] the outer flame boundary could be identified close to the edge of the visual thickness of the shear layer flames, and, therefore, the actual molecular mixing thickness was estimated to be only one-half as thick as the visual thickness.[13] The combustion efficiency obtained in these studies was uncertain and expected to lie in the range 0.5–1.0. Therefore, to increase the combustion efficiency the combustor in the present work has been lengthened to $10H$ anticipating that complete reactions would occur over this length, from considerations of flame development and thermal choking.

Important compressibility effects are associated with the shear-layer flames. The step burner flame has two flame regions connected by a presumably short transition zone. The first region is the shear layer initiated at the step between the separated, chemically reacting region and the outer, high-speed, cold airstream. Downstream of the reattachment, the favorable pressure gradient in a subsonic reacting flow accelerates the hot gases preferentially so that the burning gases are on the high-speed side of the shear layer causing the vortex roller structures to reverse direction.[14] Compressibility effects[15] tend to decrease the shear-layer growth rate by a factor of two in the fully supersonic case described here, in the absence of upstream shock interaction. This introduces an additional flow structure coupling into the experimental approach because, if the choking starts from a subsonic flow regime, the compressibility effects would be reduced. In flight the combustor would likely approach choking from supersonic conditions, and, therefore, in the present work, it was chosen to start the thermal choking process from supersonic flow. Close to thermal-choking or full thermal backpressure conditions, the compressibility effect is not large, and the effect on combustion efficiency is expected to be similar in both cases.

An additional effect, separate from compressibility, is that of shock impingement on the mixing layer or the separation region. This interaction is expected to be present when approaching choking from supersonic conditions. Huh and Driscoll[16] present flow visualization and quantitative results indicating combustion enhancement caused by shock-mixing layers interactions induced by wedges. Their data showed that the flame propagation was slow and the flow remained stratified into burned and unburned pockets over a long distance. A goal of the present work is to find out if stronger heat addition at lower Mach number can enhance the flame-spreading rate.

Because the data obtained by Pitz and Daily in Ref. 12 were based on premixed gases, other practical considerations derive from local fuel-injection distribution and the effects of a heterogeneous mixture. The recent experimental study of the effect of direct injection in bluff-body flame holders by Carrier et al.[17] shows an improved efficiency for direct injection over premixing. Therefore an important focus of the present work concerns the effects of fuel distribution on flame propagation and choking. Here, the fuel injection has been modulated, as mentioned, in two zones: 1) direct injection in the subsonic recirculation region to achieve fast heat release at low flight enthalpy and 2) from supersonic injectors in the ramps to improve mixing via axial vorticity from the supersonic side.

This brief review of prior work indicates that Mach-number and Reynolds-number differences were significant in decreasing the growth of the shear-layer flame. The molecular mixing fraction of the shear layer was dominant in reducing the expected combustion efficiency. Direct injection, pressure gradient, and shock impingement had positive effects on the predicted combustion efficiency.

Experimental Facility

The facility at the University of Florida provides direct-connect tests with a variable combustion chamber entrance Mach of 1.56–3.6 and stagnation temperatures corresponding to Mach 3.0–4.8 flight. All of the experiments presented here were performed with combustion chamber entrance Mach 1.56 and a stagnation temperature of 850 K, which represents conditions close to $M_\infty = 3.0$. The facility, shown in Fig. 1, has been described in detail elsewhere.[18] Briefly, this continuously operating, blowdown facility contains a vitiated heater based on hydrogen combustion with oxygen replenishment, electronically controlled by a fuzzy logic controller to maintain 1) constant 0.21 oxygen mole fraction at all conditions and 2) constant stagnation temperature at the heater exit as required by the experiment. A bellmouth with four-side contraction leads to the supersonic nozzle with compression on two sides, which are interchangeable nozzle blocks, to cover the range of Mach 1.56–3.6. A ceramic insulation layer added on the bellmouth entrance of the nozzle produces a larger vorticity layer in the test section on the walls without compression, as shown by nozzle calibration total pressure contours in Fig. 2. The overall pressure distribution appears to be uniform. The increased thickness of the boundary layer on the flat walls of the nozzle introduced more three-dimensionality in the test than desired. The injection ports were placed on the side with the thinner boundary layer, i.e., the

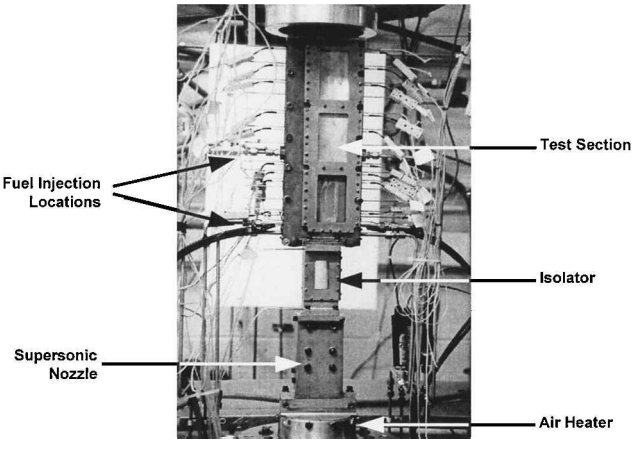

Fig. 1 Supersonic combustion facility.

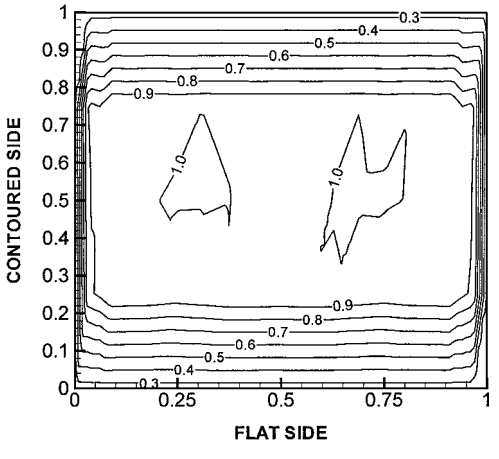

Fig. 2 Normalized stagnation pressure at isolator entrance.

nozzle contoured side. A constant-area isolator is placed between the nozzles and the combustor section to protect the nozzle flow from upstream pressure effects induced by combustion in the test section. Wall pressure ports are placed in the isolator to measure the degree of upstream interaction produced by combustion in the chamber. Optical access is available to the isolator's flow from three sides. The test section is symmetric with ample optical access through side windows. The cross section is 2.5×2.5 cm upstream of the step, and the combustion chamber total length is $26H$. A constant cross-section duct follows for $10H$ and continues with a diverging duct for the next $16H$. The flameholding and fuel-injection configuration, derived from earlier work,[19] is described in Fig. 3. The ramps are part of the step, and the step is split into positive and negative slopes to maintain a constant cross section. Gaseous-hydrogen fuel is injected by separate and independently flow-controlled systems from both the ramps and the step base. The base injection provides a method of fueling the recirculation region for flameholding and also provides the means for main heat addition.

On each side of the test section, base fuel is injected from nine 0.8-mm, sonic orifices. The ramp is fueled through two supersonic nozzles with a throat diameter of 2.4 mm. The fuel mass flow was computed by using the measured total supply pressures and temperatures and the corrected sonic area of the fuel orifice via injector discharge coefficient determined from gaseous flow.

Results

Experimental Conditions and Pressure Rise

Heat addition has been provided by fueling the base only or through combinations of base and ramp for total equivalence ratio to 0.7. Figure 4 shows the experimental points on a diagram that indicates the equivalence ratios from each injection source. Next to each experimental data point the maximum pressure rise in the constant cross-section area duct, normalized by the entrance static pressure, is shown. The accuracy of the data was within 5–6% at total equivalence ratios up to 0.4 and improving in the upper range. Up to a total equivalence ratio of around 0.35, there is no preferential pressure rise as a result of any combination of ramp vs base ratios. This trend is evident in Figs. 5a–5d, which show the normalized pressure rise vs total equivalence ratio for sets of data in which extreme ratios of Φ_{ramp}/Φ_{base} have been grouped. High mixing and combustion efficiency are expected in the low, total equivalence ratio cases. At large equivalence ratios the base injectors become more efficient. This is caused, probably, by a longer residence time available to the base-injected fuel in a low-speed, high-temperature environment in comparison with the ramp-injected fuel. The general trend indicates a drop in mixing and combustion efficiency as the total equivalence ratio increases.

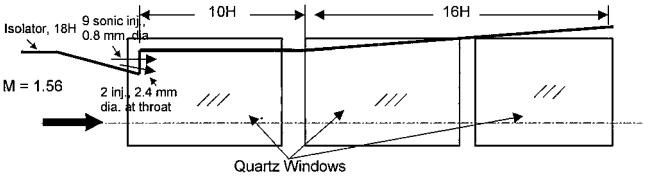

Fig. 3 Schematic of test section with injector block having nine 0.8-mm-diam sonic injectors and two 2.4-mm-diam supersonic injectors.

Wall-Pressure Distribution

Figure 6 shows wall-pressure distributions normalized by the entrance static pressure for selected combinations of fuel injection with total equivalence ratios up to 0.6. The origin of the axial coordinate has been placed at the step. Upstream pressure taps are located in the isolator duct. The plot shows higher pressure rise obtained when fuel injection from the base is preponderent.

The static-pressure distribution has a maximum value near the center of the combustor constant-area section and is associated with the reattachment location of the flow over the step. Downstream the pressure drops quickly and continuously through the constant-area combustor and into the expansion section until near the end where separation shocks occur to match the local ambient pressure.

Acceleration of the air in both the second half of the constant-area duct, i.e., beyond $5H$, and the expansion duct indicates supersonic expansion section flow. The presence of low-speed, subsonic-burning layers in the vicinity of the walls,[20] as indicated schematically in the figure, generates a convergent–divergent channel in which the core flow remains supersonic throughout the constant area of the test section and then continues to expand in the divergent section. As a result, the favorable pressure gradient tends to decrease the shear-layer growth in the fully supersonic case of these experiments, in which upstream shock interactions were not present.

The maximum isolator pressure rise caused by blockage in the test section was obtained by physical blocking of the exit of the expanding section in a nonreacting flow. The axial pressure distribution results for the blocking tests is shown in Fig. 7. The maximum pressure rise is 2.1 at the end of the constant-area section at the onset of upstream interaction. This pressure is achieved before further upstream interactions with the nozzle flow occur. Based on this pressure in the base, a one-dimensional calculation indicates an expected ideal choking equivalence ratio $\phi = 0.5$.

Because the pressure distribution in the $18H$ long isolator, at negative axial locations in Fig. 6, does not show any differences from one case to the other with heat addition, it is estimated that the isolator flow was, probably, attached at the step.

Figure 8 shows the combustion efficiency calculated with a simplified, one-dimensional analysis that estimated the amount of heat release required to produce the pressure rise measured at each axial

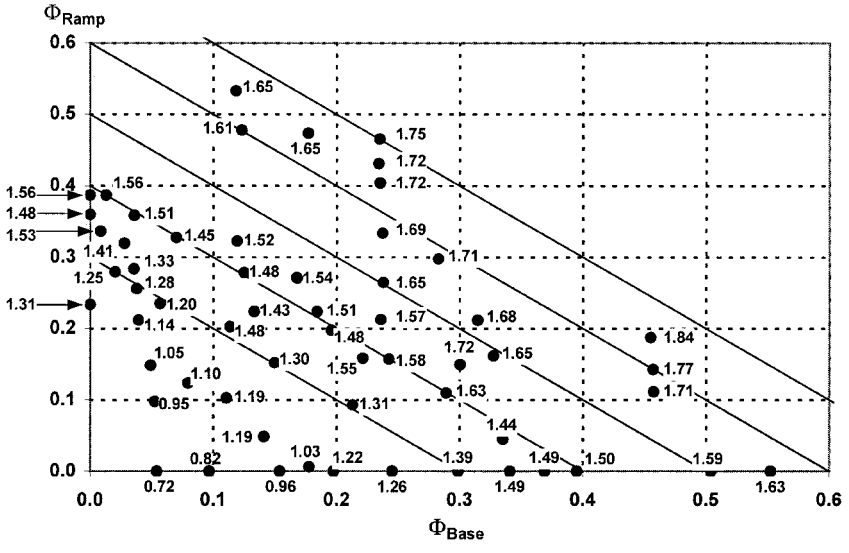

Fig. 4 Effect of fuel-injection distribution mode (base/ramp) on $(P_{wall} \lhd P_s)_{max}$.

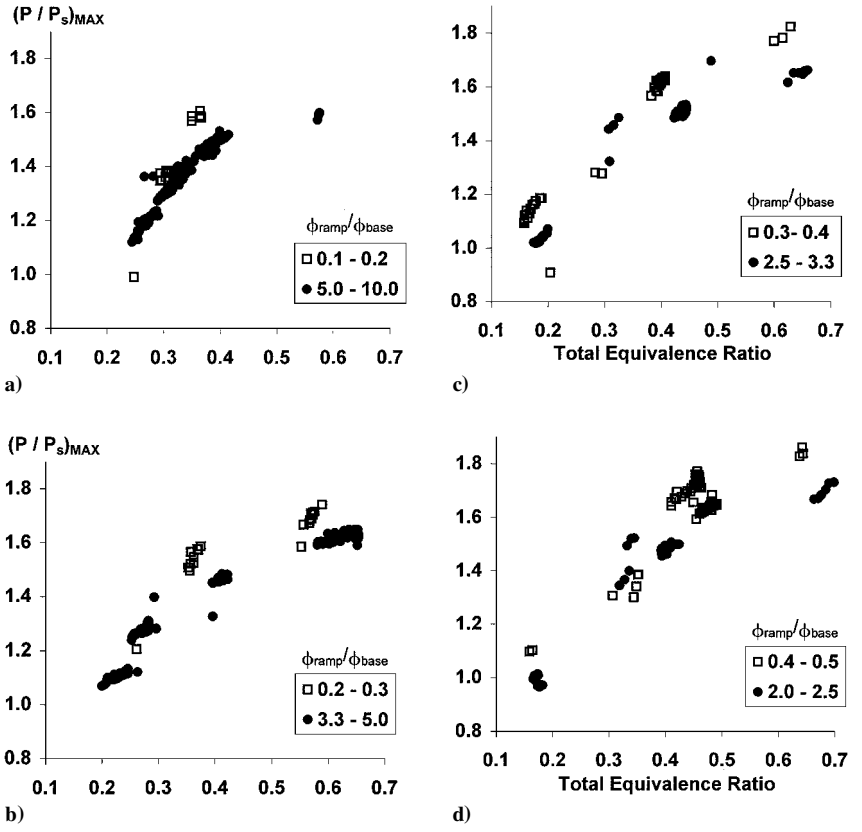

Fig. 5 Normalized pressure rise vs Φ_{total} with different fuel-injection distribution ratios ($\Phi_{ramp} \lhd \Phi_{base}$).

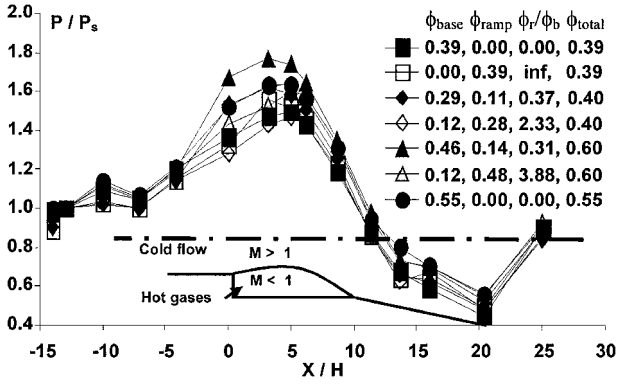

Fig. 6 Streamwise test section pressure profile (normalized) for $\Phi_{total} = 0.60$, showing flow acceleration and absence of thermal choking.

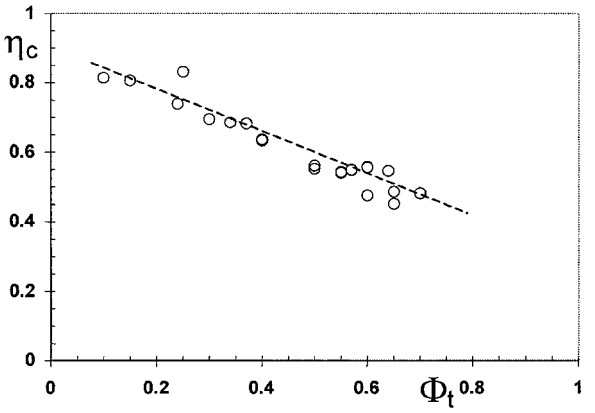

Fig. 8 Combustion efficiency based on wall pressures with one-dimensional analysis.

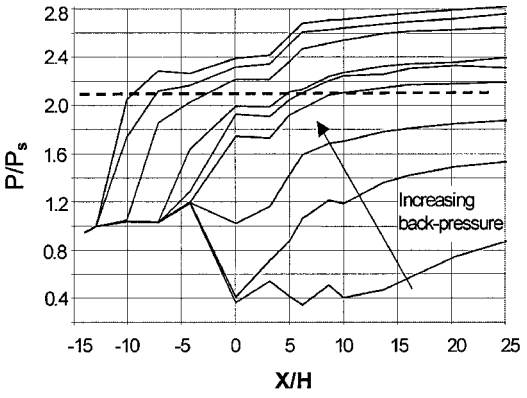

Fig. 7 Test-section pressure profile with increasing backpressure for a nonreacting flow.

location, under assumptions of 100% mixing. The combustion efficiency has been estimated in this plot at the end of the constant-area duct. As noted, under the assumptions of complete mixing and combustion this pressure rise would be achieved with an equivalence ratio close to 0.5. As the efficiency dropped with increased total equivalence ratio, operation with $\phi = 0.7$ resulted in stable and controllable combustion without thermal choking. The analysis shows a definite transition from a relatively high level of performance up to an equivalence ratio of 0.1 to a lower level at $\Phi = 0.5$. The estimated combustion efficiency, which incorporated both chemical kinetics and mixing effects, was about 60% at $\phi = 0.5$, further dropping as the total equivalence ratio increased. This reduction in combustion efficiency was attributed to reduced mixing and is not expected for normally propagating flames for which flame spreading should increase as heating decelerates the entering air.

An additional measure of combustion efficiency is given by the pressure rise in the base normalized by the entrance static pressure, shown in Fig. 9 along with the theoretical pressure rise if

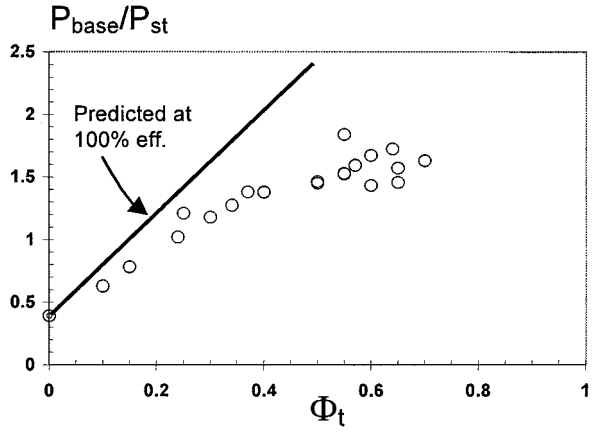

Fig. 9 Pressure rise in the step base vs predicted ideal efficiency curve.

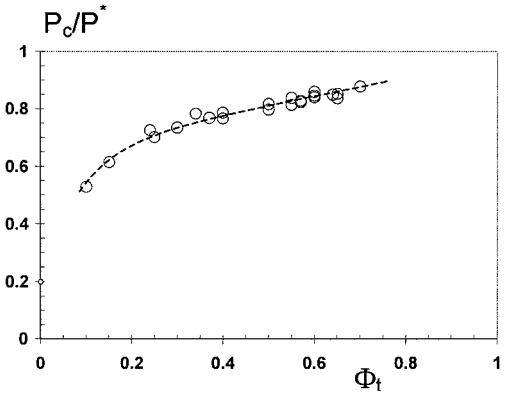

Fig. 10 Maximum pressure rise normalized by required choking pressure indicating unchoked flow.

combustion were complete with 100% mixing and burning. The same degradation of combustion efficiency as the equivalence ratio increases is observed.

A nozzle stream thrust calculation based on the total airflow and the pressure at the nozzle entrance, which accounts for the fuel thrust and the thrust generated on the base, can be estimated on the assumption of uniform conditions as

$$F_c = \dot{m}_{\text{air}} \cdot V_n + P_n \cdot A_n + P_{\text{base}} \cdot A_{\text{base}} + \sum_i \dot{m}_{\text{fuel}_i} \cdot V_{\text{fuel}_i}$$

where $\dot{m}_{\text{air}}$ and $\dot{m}_i$ represent the air and fuel flow rates, respectively; V_n and V_i represent the velocities of the air at the entrance into the combustion chamber and the fuel velocities, respectively; A_n is the entrance area, and A_{base} is the base frontal area. This stream thrust can, then, be used to determine a theoretical choking pressure, as follows:

$$P^* = F_c / A_c(1+\gamma)$$

where A_c is the area at the exit of the combustor and γ is the ratio of the specific heats, estimated in this calculation based on equivalence ratio. Figure 10 shows the ratio of the pressure at the exit of the constant-area duct normalized by the calculated choking pressure indicating that for the current experimental conditions the flow was supersonic at the combustor exit. The figure shows that only about 80% of this pressure was attained at $\phi = 0.5$. Above $\phi = 0.5$ only small increments in the pressure rise were noted with further fuel addition caused, largely, by decreased mixing efficiency for the ramp injectors and chemical kinetics effects for the base injectors. The measured exit pressures were converted to Mach number shown in Fig. 11. This Mach number indicates the proximity to choking and the combustion efficiency and is an important parameter for estimating the compressibility effects on the flame propagation rate at the exit.

The combustion efficiency estimated from the measured data was lower than expected, based on the results of Ref. 12. However, the

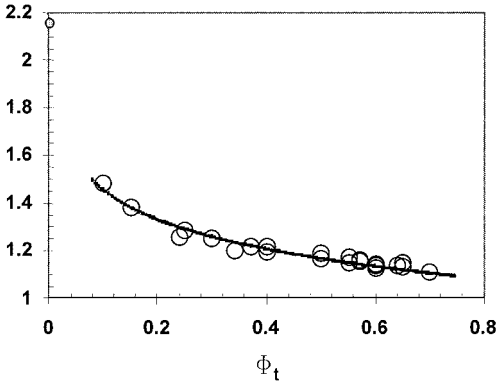

Fig. 11 Combustor exit Mach number indicates unchoked flow at maximum Φ_{total} attained (temp. limited).

combustion efficiency falls at the low end of the prediction based on the analysis of the normal shear-layer flame compressibility and Reynolds-number effects. The basic assumption of short mixing length for the hydrogen fuel jets in this analysis, namely complete mixing, can cause the differences. At large equivalence ratios the large fuel molar fraction and dynamic pressure ratio at the injection station can cause the fuel jets to penetrate through the recirculation region. Mixing will occur, then, at significant closer gases-fuel velocities, i.e., from ~0 in the recirculation region to ~0.8 beyond, thus reducing the development of the shear layer and resulting in an estimated reduction of the mixing rate to 25% of the combustion efficiency analysis already presented. Thus a combination of fuel stratification and compressibility effects accounts for the difference between the expected and measured combustion efficiencies. This estimate is corroborated by flame extinction experiments and was found to correlate with gas dynamics rather than chemical kinetics effects,[21] when at an equivalence ratio of 0.1 a sudden transition takes place as a result of gas dynamics effects.

Statistical High-Equivalence-Ratio Prediction

Using optimization techniques based on analysis of variance,[22] a two-dimensional function has been fitted to the measured pressure rise data to predict the pressure rise for higher equivalence ratios at conditions that impose severe thermal stress on the device. Based on a large number of results obtained with relatively low equivalence ratios and only a few results with high equivalence ratios, this function offers a first order predictive tool for conditions of high equivalence ratios, thus providing guidance for the experiment. This function is given by the following equation:

$$P_r = \left(A + \frac{a_1}{(0.01+\Phi_b)^3} - \frac{a_2}{(0.01+\Phi_b)^2} + \frac{a_3}{0.01+\Phi_b} + \frac{b_1}{(0.01+\Phi_r)^3} - \frac{b_2}{(0.01+\Phi_r)^2} + \frac{b_3}{0.01+\Phi_r} - \frac{c_1}{(0.01+\Phi_b)(0.01+\Phi_r)^2} - \frac{c_2}{(0.01+\Phi_b)^2(0.01+\Phi_r)} + \frac{c_3}{(0.01+\Phi_b)(0.01+\Phi_r)} \right)^{-1}$$

where P_r is the constant-area exit pressure rise normalized by the entrance pressure, Φ_b and Φ_r are the equivalence ratios for the base and the ramp, respectively; and the coefficients resulted from fitting the equation to the data base, as follows:

$$A = 0.382876, \qquad a_1 = 2.63963 \times 10^{-6}$$
$$a_2 = 4.28383 \times 10^{-4}, \qquad a_3 = 1.64088 \times 10^{-2}$$
$$b_1 = 1.58438 \times 10^{-5}, \qquad b_2 = 2.01042 \times 10^{-3}$$
$$b_3 = 4.27530 \times 10^{-2}, \qquad c_1 = 4.36712 \times 10^{-6}$$
$$c_2 = 6.22650 \times 10^{-6}, \qquad c_3 = 1.27155 \times 10^{-3}$$

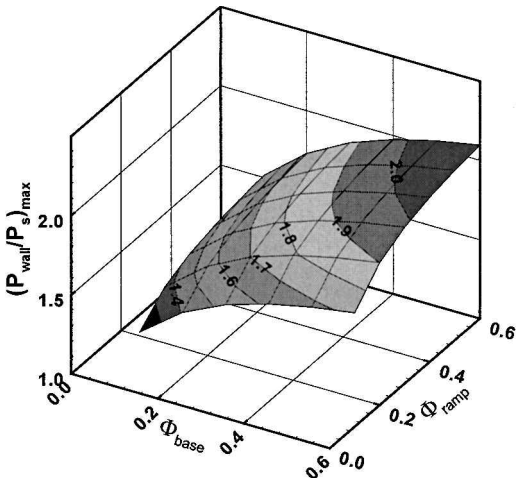

Fig. 12 Predicted pressure rise with fuel-injection distribution showing effective base injection mode.

Using this expression, the pressure-rise prediction is given in Fig. 12, indicating that thermal choking at the end of the constant-area duct would be obtained in this configuration at near stoichiometric conditions. The predicted base-pressure rise would, then, reach a value of about 2.1, which in the nonreacting, backpressurizing experiments was the highest pressure rise attained before upstream nozzle interactions were noted. The statistical analysis is consistent with one-dimensional gas dynamics analysis.

Summary

A combined fuel-injection scheme with gaseous-hydrogen modulation between two injection zones in supersonic flow, indicated the following:

1) When the total equivalence ratio remained under moderate values, i.e., $\phi = 0.35$, no preferential injection mode was noticed to produce a higher combustion efficiency, as reflected by the combustion chamber pressure rise. At large, total equivalence ratio injection through the base produced a larger pressure rise as a result of an increased residence time in comparison with the ramp-injected fuel.

2) Within the duct's constant-area section the slow-speed, burning layer originating in the base of the flameholder creates a combustor blockage that takes the shape of a convergent-divergent channel. As a result, the maximum pressure rise is close to the middle of the constant-area duct, and the core flow accelerates in the divergent part. The presence of an expanding section following the constant-area duct further accelerates the flow and reduces the pressure in the axial direction. Thus, the favorable pressure gradient tends to decrease the shear-layer growth in the fully supersonic case of these experiments, in which upstream shock interactions were not present.

3) Gradual blockage of a nonreacting flow resulted in a pressure rise in the constant-area section of the duct, with a pressure ratio of 2.1 noted at the onset of upstream interaction.

4) Under the assumptions of complete mixing and combustion, this pressure rise would be achieved with an equivalence ratio close to 0.5. As the efficiency dropped with increased total equivalence ratio, operation with $\phi = 0.7$ resulted in stable and controllable combustion without thermal choking.

5) The transition from near complete combustion to lower combustion efficiency occurred within the range of $\phi = 0.1 - 0.5$ with further drop of efficiency for higher equivalence ratio.

6) From estimates of stream thrust, a theoretical choking pressure has been calculated, indicating that only about 80% of this pressure was attained at $\phi = 0.5$. Above $\phi = 0.5$ only small increments in the pressure rise were noted with further fuel addition caused, largely, by decreased mixing efficiency for the ramp injectors and chemical kinetics effects for the base injectors.

7) As a result, the estimated combustion efficiency, which incorporated both chemical kinetics and mixing effects, was about 60% at $\phi = 0.5$, further dropping as the total equivalence ratio increased.

Acknowledgments

The authors are grateful to Raphael Haftka, University of Florida, who provided the technique for the prediction of combustion chamber pressure rise at high equivalence ratios. This work has been supported by Boeing Defense and Space Group.

References

[1]Owens, M. G., Tehranian, S., Segal, C., and Vinogradov, V. A., "Flameholding Configurations for Kerosene Combustion in a Mach 1.8 Airflow," *Journal of Propulsion and Power*, Vol. 14, No. 4, 1998, pp. 456–461.

[2]Waitz, I. A., Marble, F. E., and Zukovski, E. E., "Vorticity Generation by Contoured Wall Injectors," AIAA Paper 92-3550, July 1992.

[3]Kraus, D. K., and Cutler, A. D., "Mixing Enhancement by Use of Swirling Jets," AIAA Paper 93-2922, June 1993.

[4]Sabelnikov, V. A., Voloschenko, O. V., Ostras, V. N., Sermanov, V. N., and Walther, R., "Gasdynamics of Hydrogen-Fueled Scramjet Combustors," AIAA Paper 93-2145, June 1993.

[5]Vinogradov, V., Kobigsky, S., and Petrov, M., "Experimental Investigation of Liquid Carbonhydrogen Fuel Combustion in Channel at Supersonic Velocities," AIAA Paper 92-3429, July 1992.

[6]Baurle, R. A., Fuller, R. P., White, J. A., Chen, T. H., Gryber, M. R., and Nejad, A. S., "An Investigation of Advanced Fuel Injection Schemes for Scramjet Combustion," AIAA Paper 98-0937, Jan. 1998.

[7]Northam, G. B., Greenberg, I., Byington, C. S., and Capriotti, D. P., "Evaluation of Parallel Injector Configurations for Mach 2 Combustion," *Journal of Propulsion and Power*, Vol. 8, No. 2, 1992, pp. 491–499.

[8]Hartfield, R. J., Hollo, S. D., and McDaniel, J. C., "Experimental Investigation of a Swept Ramp Injector Using Laser-Induced Iodine Fluorescence," *Journal of Propulsion and Power*, Vol. 10, No. 1, 1994, pp. 129–135.

[9]Riggins, D. W., McClinton, C. R., Rogers, R. C., and Bittner, R. D., "Investigation of Scramjet Strategies for High Mach Number Flows," *Journal of Propulsion and Power*, Vol. 11, No. 3, 1995, pp. 409–418.

[10]Stouffer, S. D., Baker, N. R., Capriotti, D. P., and Northam, G. B., "Effects of Compression and Expansion-Ramp Fuel Injector Configuration on Scramjet Combustion and Heat Transfer," AIAA Paper 93-0609, Jan. 1993.

[11]Ganji, A. R., and Sawyer, R. F., "Experimental Study of the Flowfield of a Two-Dimensional Premixed Turbulent Flame," *AIAA Journal*, Vol. 18, No. 7, 1980, pp. 817–824.

[12]Pitz, R. W., and Daily, J. W., "Combustion in a Turbulent Mixing Layer Formed at a Rearward-Facing Step," *AIAA Journal*, Vol. 21, No. 11, 1983, pp. 1565–1570.

[13]Dimotakis, P. E., "Turbulent Free Shear Layer Mixing and Combustion," *High-Speed Flight Propulsion Systems*, edited by S. N. B. Murthy and E. T. Curran, Vol. 137, Progress in Astronautics and Aeronautics, AIAA, Washington, DC, 1991, pp. 89–126.

[14]Wright, R. H., and Zukoski, E. E., "Flame Spreading from Bluff Body Flameholders," Jet Propulsion Lab., Technical Release no. 34-17, Pasadena, CA, May 1960.

[15]Papamoschou, D., and Roshko, A., "The Compressible Turbulent Shear Layer: An Experimental Study," *Journal of Fluid Mechanics*, Vol. 197, No. 4, 1988, pp. 453–477.

[16]Huh, H., and Driscoll, J. F., "Measured Effects of Shock Waves on Supersonic Hydrogen-Air Flames," AIAA Paper 96-3035, July 1996.

[17]Carrier, D., DeChamplain, A., and Bardon, M., "Direct Fuel Injection for Bluff Body Flame Stabilization," AIAA Paper 96-3032, July 1996.

[18]Segal, C., and Young, C. D., "Development of an Experimentally-Flexible Facility for Mixing-Combustion Interactions in Supersonic Flow," *Journal of Energy Resources Technology*, Vol. 118, No. 2, June 1996, pp. 152–158.

[19]Ortwerth, P., Mathur, A., Vinogradov, V. A., Grin, V., Goldfeld, M., and Starov, A., "Experimental and Numerical Investigation of Hydrogen and Ethylene Combustion in a Mach 3-5 Channel with a Single Injector," AIAA Paper 96-3245, July 1996.

[20]Strokin, V., and Grachov, V., "The Peculiarities of Hydrogen Combustion in Model Scramjet Combustion," *Proceedings of the 13th International Symposium on Airbreathing Engines Symposium*, edited by Frederick S. Billig, AIAA, Reston, VA, 1997, pp. 374–384.

[21]Ortwerth, P. J., Mathur, A. P., Segal, C., Mullagilli, S., and Owens, M. G., "Combustion Stability Limits of Hydrogen in a Non-Premixed, Supersonic Flow," *Proceedings of the 14th International Symposium on Airbreathing Engines Symposium*, edited by Paul Waltrup, AIAA, Reston, VA, CD-ROM, Paper ISABE 99-7136, 1999.

[22]Myers, R. H., and Montgomery, D. C., *Response Surface Methodology*, Wiley, New York, 1995, pp. 294–297.